in a closed loop (our ASE method). We get flight conditions for ASE analysis in a closed loop that are identical to those used by STARS.[1]

The flutter speeds obtained with our three methods, namely, 1) the flutter p method, 2) the LS forces approximation applied on the flutter p method (our ASE p&LS method), and 3) the MS2LS unsteady forces approximation applied on the flutter p method, were found to be very close to each other (values of around 260 kn). The slight difference is explained by the precision of LS or MS2LS methods applied to the ATM.

Conclusions

Four types of analyses were conducted on the ATM to characterize flutter in the ASE context. ASE analysis by the pk method first introduced the ATM and verified the pertinence of its data and the results obtained by STARS software at the NASA DFRC.[1] In fact, a comparative study of the values of aeroelastic analysis applied on the ATM by the pk method and the aeroelastic results with STARS revealed good coherence at the level of flutter prediction in an open loop. After this analysis, the ATM was found to be consistent.

ASE analysis on the ATM by the p method in a closed loop allowed the validation of its ability to represent complex ASE systems and to predict the flutter phenomenon in closed-loop ASE systems. Comparative study of the results of ASE analysis applied on the ATM by the p method, and of the ASE values in STARS, revealed a prediction relatively identical to a flutter phenomenon in a closed loop very close to 260 kn. This analysis shows the importance of taking the chain of control, the dynamics of actuators, and the sensors in the flutter prediction phenomenon into account, as suggested by the p method in a closed loop, because the flutter phenomenon appears at a much weaker speed in a closed loop (263 kn) than it does in an open loop (441 kn). Finally, the two last analyses allowed us to test the impact of aerodynamic forces approximated by the LS or MS2LS methods on flutter phenomenon prediction, first in an aeroelastic context, and later on in an ASE context. Also, aerodynamic forces approximation used in the analyses, which consists of LS minimization, is not optimal. The precision of aerodynamic forces approximation may be increased significantly by augmention of the number of aerodynamic lags on the one hand, or by the use of the most powerful approximation methods that guarantee good precision by decreasing the number of aerodynamic modes on the other. Detailed validation of an ASE analysis method is presented in this Note as is a new conversion of the MS into the LS form called MS2LS.

Acknowledgments

The authors thank Kajal Gupta of the NASA Dryden Research Flight Center for permission to use the aircraft test model in STARS. Thanks are also due to other members of the STARS Engineering Group for their continuous assistance and collaboration: T. Doyle, M. Brenner, C. Bach, and S. Lung.

References

[1]Gupta, K. K., "STARS—An Integrated, Multidisciplinary, Finite-Element, Structural, Fluids, Aeroelastic, and Aeroservoelastic Analysis Computer Program," NASA TM-101709, 1997.

[2]Noll, T., Blair, M., and Cerra, J., "ADAM, An Aeroservoelastic Analysis Method for Analog or Digital Systems," *Journal of Aircraft,* Vol. 23, No. 11, 1986, pp. 852–858.

[3]Adams, W. M., and Hoadley, S. T., "ISAC: A Tool for Aeroservoelastic Modeling and Analysis," NASA TM-109031, 1993.

[4]Pitt, D. M., and Goodman, C. E., "FAMUSS—A New Aeroservoelastic Modeling Tool," AIAA Paper 92-2395, 1992.

[5]Karpel, M., "Reduced-Order Models for Integrated Aeroservoelastic Optimization," *Journal of Aircraft*, Vol. 36, No. 1, 1999, pp. 146–155.

[6]McLean, D., *Automatic Flight Control Systems*, Series in Systems and Control Engineering, Prentice–Hall International, Cambridge Univ. Press, Cambridge, England, U.K., 1990, Chaps. 2–4.

Thick Wings in Steady and Unsteady Flows

Reza Karkehabadi*
Lockheed Martin/NASA Langley Research Center, Hampton, Virginia 23681

Introduction

SOLUTIONS of full Navier–Stokes equations for three-dimensional bodies in unsteady flowfields are challenging. One method that is available to compute the unsteady flowfields for arbitrary bodies is the unsteady vortex-lattice method (UVLM). When the pressure distribution on a thick wing is not required and the lift and moment coefficients are sufficient, often a thick wing is replaced by a lifting surface. By this approximation, one can realize substantial reductions in computational time. The question is when such an approximation appropriate and how thick of a wing can be replaced by a lifting surface? In this Note, the effect of thickness on the aerodynamic lift and moment is investigated. The general, unsteady, three-dimensional, vortex-lattice method is evaluated by making a number of comparisons between numerical results obtained from UVLM and experimental data. The pressure coefficient of a thick wing using UVLM is compared to the exact solution. Both steady and unsteady flows are considered, and both thick-wing and lifting-surface versions of UVLM are used.

Analysis

When a wing of arbitrary planform is set in motion, vorticity is generated in a thin region adjoining the surface known as the boundary layer. Some of this vorticity is shed into the flow and becomes the wake. It follows from the definition of vorticity that vorticity anywhere in the flowfield induces velocity everywhere in the flowfield. This is a kinematical result and valid for viscous as well as inviscid flows. In the actual flow, the vorticity-induced disturbance emanating from the boundary layers and wake interfere with the oncoming stream to the extent that both the no-slip and no-penetration boundary conditions are satisfied on the surface of the wing.

In the present aerodynamic model, vortex sheets wrapped over the body surfaces simulate the boundary layers. These infinitesimally thin layers of vorticity may be viewed as the infinite Reynolds number approximation of the actual boundary layer. Hence, one can expect the present model to improve as the Reynolds number increases. To expedite the calculation of the induced-velocity field, the sheets are replaced by lattices of discrete vortex lines. Each line segment in the lattice is relatively short and straight, and its induced velocity is readily calculated from the familiar Biot–Savart law.

The circulations around the individual segments of the lattice are determined by imposing simultaneously the no-penetration condition at the centroid of the corners in each element and spatial conservation of circulation. For the pressures on the upper and lower surfaces of the body along the sharp trailing edges to be the same, vorticity must be shed. This shed vorticity is convected away from the wing and constitutes the wake. The flow is irrotational everywhere except in the boundary layer of the body, where vorticity is being generated, and in the wake. The flow in the wake is considered to be inviscid and rotational; hence, to make the wake force free, the vorticity is convected with the fluid particles. The present method

Received 14 August 2003; revision received 10 February 2004; accepted for publication 11 February 2004.

*Staff Engineer, Aerodynamics, Structures, and Materials Department. Member AIAA.

predicts the shape and the distribution of vorticity in the wake as part of the solution. In satisfying the no-penetration condition and in convecting the wake, the velocity field induced by the wake is taken into account.

The UVLM was used for wings in oscillation by Karkehabadi and Mook.[1] In their work, a lifting surface was used for a cambered airfoil. In the present work, the unsteady vortex lattice method is applied to lifting surface and thick wings. The pressure coefficient is calculated from the familiar Bernoulli equation for unsteady flows. To calculate the derivative of the velocity potential, the value of the velocity potential is needed at every time step. For an irrotational flow,

$$\boldsymbol{V} = \nabla\phi \tag{1}$$

The unknown values of ϕ for a thick wing on every element of the body at a given instant were obtained by numerically integrating

$$\phi(\boldsymbol{r}) - \phi(\boldsymbol{r}_0) = \int_{r_0}^{r} \boldsymbol{V}(\boldsymbol{r}) \cdot \mathrm{d}\boldsymbol{r} \tag{2}$$

where $\boldsymbol{r}_0$ is an arbitrary starting point and $\boldsymbol{V}$ is the velocity of the fluid particle. The time derivative is computed from a finite difference formula. For more detailed derivation of the formula for thick wings, the reader is referred to author's doctoral dissertation.[2]

When the wing is thin, the vortex sheets on the upper and lower surfaces are merged into a single lifting surface at the camber line. The force on each element of the bound lattice is calculated by determining the pressure jump across the lifting surface and multiplying it by the area of the element. The value of the velocity potential is required at every time step. In the term $\phi_u - \phi_l$, the subscripts u and l denote quantities evaluated on the upper and lower surfaces. This term can be expressed in terms of the circulation of the bound lattice elements. For more information and formulations of the thin wings the reader is referred to Konstadinopoulos et al.[3]

Results

To establish credibility of UVLM for thick wings, a von Kármán–Trefftz airfoil was selected. The exact steady-state solution of a von Kármán–Trefftz airfoil is shown in Fig. 1a. Figure 1a shows the pressure coefficients at the upper and lower surface of the airfoil. Figure 1a is compared with the results obtained from UVLM. Figures 1b–1d show the pressure coefficients at the midspan of wings with different aspect ratios. These wings have the same cross

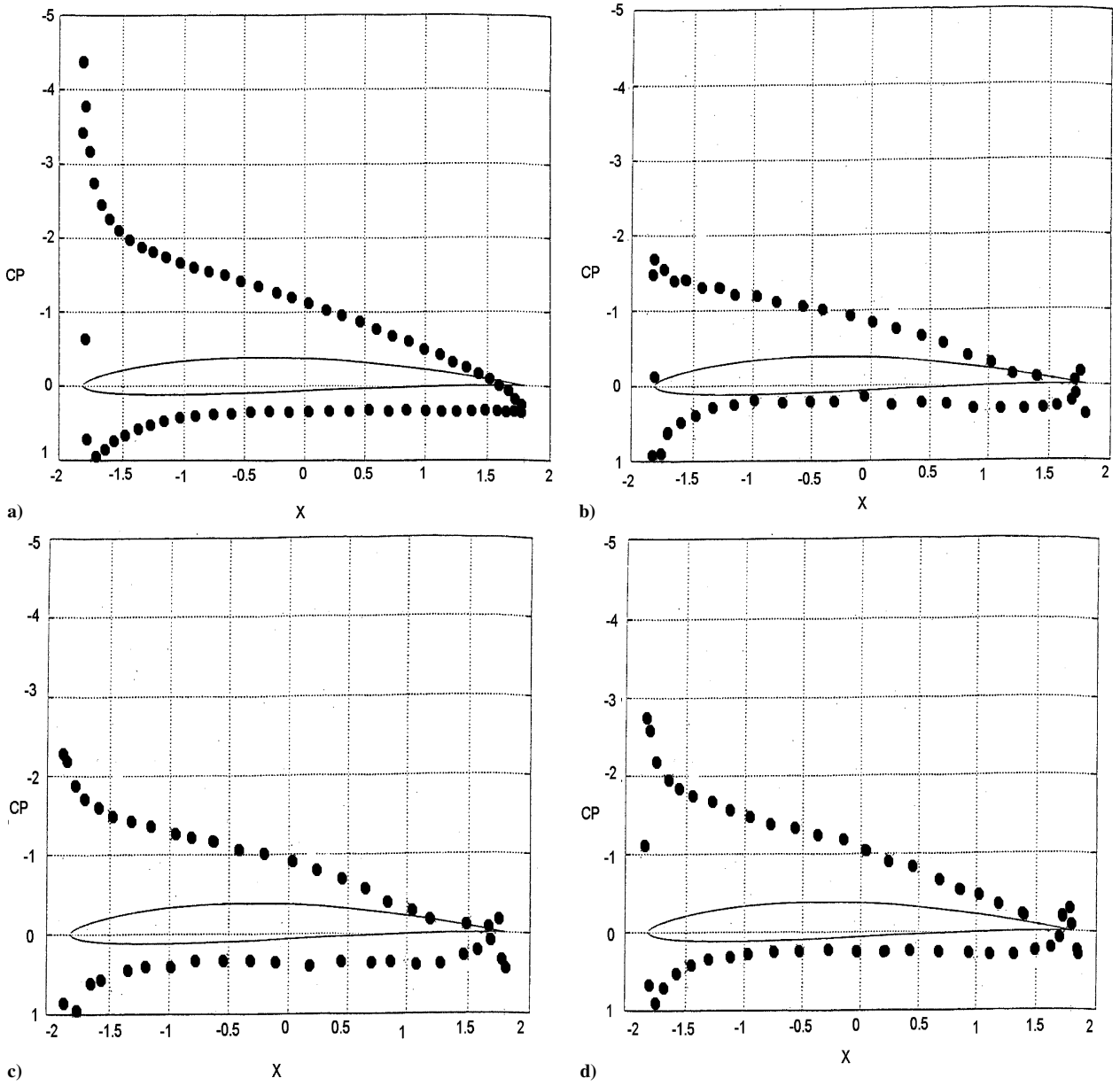

Fig. 1 Calculated pressure distributions for flow over a von Kármán–Trefftz airfoil, 8-deg angle of attack: a) exact steady-state solution, b) aspect ratio of 5.5, c) aspect ratio of 11, and d) aspect ratio of 16.6.

section but differ in aspect ratio. As Figs. 1b–1d indicate, the numerical results get closer to the exact solution as the aspect ratio increases. The unsteady results are shown after the wing has traveled 25 chords. There is better agreement with the exact steady-state solution when the wing travels farther. Another factor that affects the accuracy of the results is the time step. It affects the pressure coefficients everywhere on the wing, but especially near the trailing edge. Moreover, the time step determines the size of the elements in the wake. Therefore, the value used in the calculation has to allow a smooth transition in the size of the elements from the wing to the wake and still be small enough to provide a time-accurate solution. As the value of the time step decreases and the aspect ratio increases, the comparison with the exact solution improves.

In Fig. 2, the calculated wake using UVLM is shown. The aspect ratio for this wing is 5.5. Figure 2 shows the curling of vortices due to the impulsive start. Although vortices are not shed from the wing tip, the wake does curl along its streamwise edges, and these vortices have some effect on the pressure at mid span. As the angle of attack increases, these vortices become stronger, and they have more influence on the pressures at midspan. As the aspect ratio increases, the influence of these vortices on the pressure coefficients at midspan is reduced.

The numerical results for symmetric airfoils of different thicknesses are compared with the experimental data. Figure 3 shows a comparison of the numerical result with the experimental data for NACA 0015 (Ref. 4). The results are calculated for a flat plate and wings of different thicknesses with an aspect ratio of 30. The agreement of the present results with the experimental data for NACA 0015 is excellent. The lift and moment coefficients are in close agreement until separation occurs. As the thickness of the wing increases, the lift coefficient increases; however, the wing has to be rather thick for the thickness to make a significant contribution to the lift and moment coefficients. Note that this difference in the lift coefficient increases with the angle of attack. Figure 4 shows a comparison of the numerical result with the experimental data for a cambered airfoil, NACA 4415. Figure 4 shows close agreement to about 10-deg angle of attack for lift coefficient and excellent agreement with the moment coefficient up to where the separation occurs. The comparison of the present result with the experimental data improves as the Reynolds number increases.

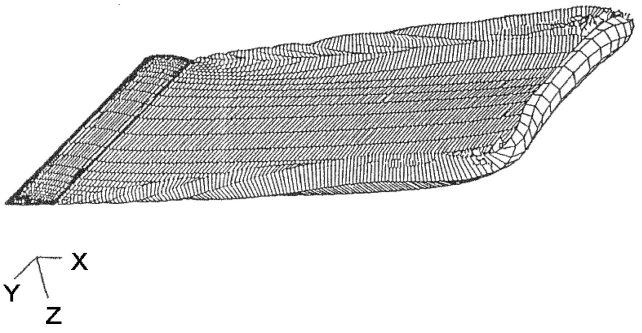

Fig. 2 Calculated wake from the UVLM for a wing with aspect ratio of 5.5 and 8-deg angle of attack.

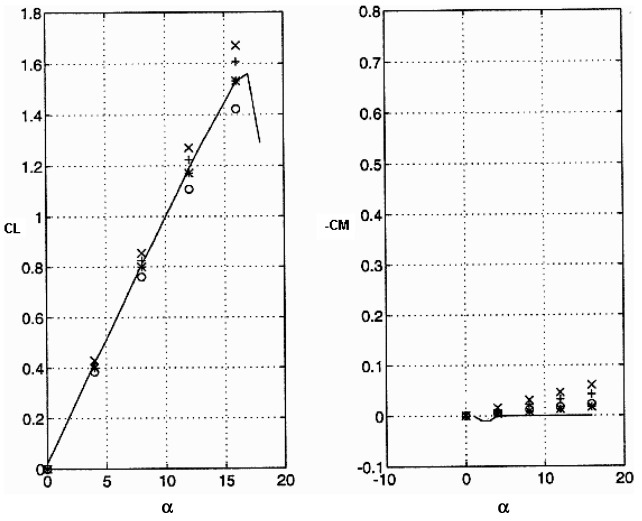

Fig. 3 Lift and moment as functions of angle of attack for uncambered airfoils of different thicknesses with aspect ratio = 30, experimental data (Miley[4]), NACA 0015 airfoil, Reynolds number 3.3 × 10^6, NACA variable density tunnel: ○, lattice method applied to 0000; ∗, lattice method applied to 0015; +, lattice method applied to 0021; and ×, lattice method applied to 0027.

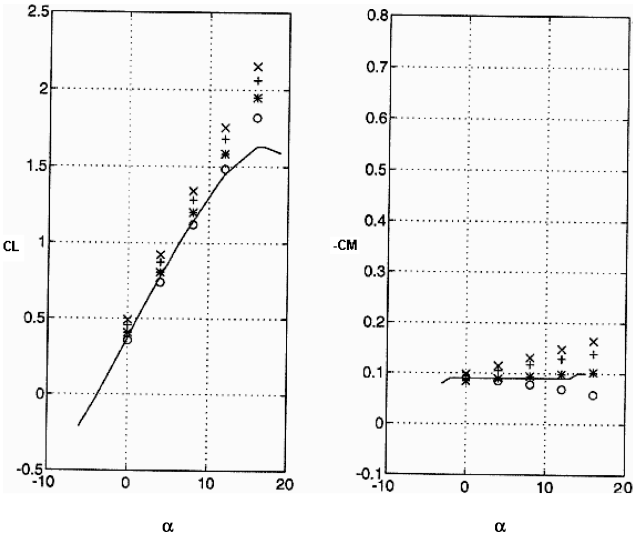

Fig. 4 Lift and moment as functions of angle of attack for cambered airfoils of different thicknesses with aspect-ratio = 30, experimental data (Miley[4]), NACA 4415 airfoil, Reynolds number 3.0 × 10^6, NACA VDT tunnel: ○, lattice method applied to 4400; ∗, lattice method applied to 4415; +, lattice method applied to 4421; and ×, lattice method applied to 4427.

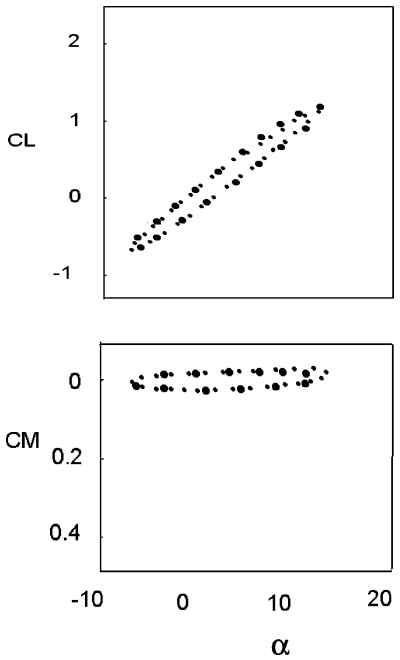

Fig. 5 Experimental and numerical lift, $\alpha = 3$ deg + 10 deg sin ωt, and moment coefficients as functions of angle of attack, NACA 0012, and $k = 0.1$; moment taken about quarter chord from the leading edge: ●, present solution, 0.055 time step and •, experimental data of McCroskey et al.[5]

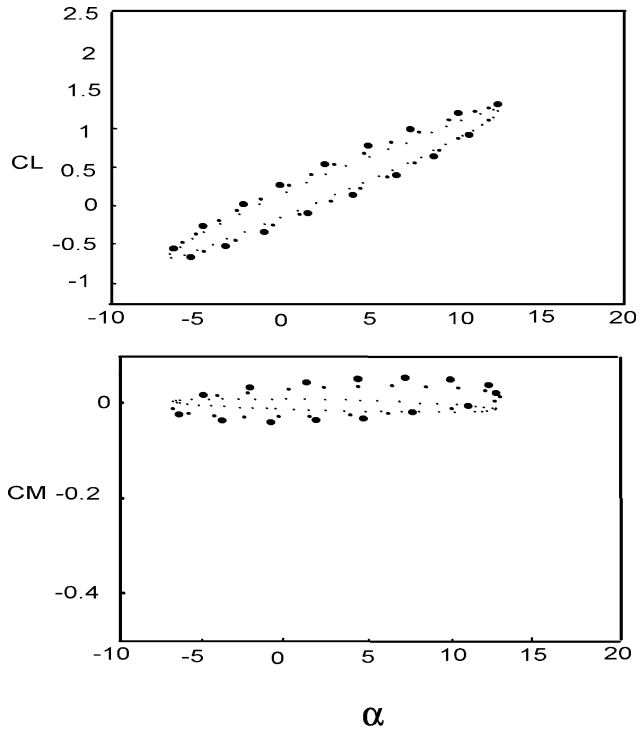

Fig. 6 Calculated lift and moment coefficients as functions of angle of attack for wings of different thicknesses, $\alpha = 3$ deg + 10 deg sin ωt, and $k = 0.1$; moment taken about quarter chord from the leading edge: ●, NACA 0027; •, NACA 0021; and ·, NACA 0012.

It is important and valuable to apply this method to unsteady problems. An airfoil with oscillation is considered here, and the calculated results are compared with the experimental data. This method was used to calculate the loads on a NACA 0012 profile with an aspect ratio of 30, oscillating sinusoidally in pitch about the quarter chord. In this example, the mean angle of attack is 3 deg, the time step is 0.055, and the amplitude of the oscillation is 10 deg. The reduced frequency, defined as $k = \omega C/2V_\infty$, is 0.1.

Figure 5 shows a comparison of the midspan aerodynamic load of the numerical results with the experimental data of McCroskey et al.[5] McCroskey et al. also gave results for higher angles of attack that produced separation. The results clearly show hysteresis associated with the periodic oscillations. The result for this wing was independently calculated by Katz and Plotkin[6] and compared with the experimental data. The calculated moment in their work is close to the experimental result with small rotation. They indicate that this is due to inaccuracy of computing the airfoil's center of pressure. This inaccuracy is present because only nine chordwise panels were used. In the present work, effort was made to obtain a better agreement with the experimental data by using more elements, particularly near the trailing edge, and using a small time step. The result from the present work is in close agreement with the experimental data.

To investigate the effect of the thickness of a wing in oscillation, the numerical results for various thicknesses are presented in Fig. 6. The predicted lift is slightly affected by the thickness; the predicted moment is more sensitive to the thickness. However, to illustrate this we had to go as high as 27%. The widening of the hysteresis loops indicates that a thick profile would dissipate more energy during a cycle.

Conclusions

The general UVLM can model wings in steady and unsteady flows. The method is capable of giving accurate pressure distributions on thick lifting bodies in both steady and unsteady flowfields. The method is sensitive to the time step and the number of elements used in the calculation. A thick wing can often be replaced by a lifting surface lying on the camber surface of the actual airfoil. This appears to be true for both steady and unsteady flowfields.

References

[1]Karkehabadi, R., and Mook, D. T., "Wing in Heaving Oscillatory Motion," *Journal of Aircraft*, Vol. 33, No. 5, 1996, pp. 913–918.

[2]Karkehabadi, R., "Numerical Simulations of Wings in Unsteady Flows," Ph.D. Dissertation, Dept. of Engineering Science and Mechanics, Virginia Polytechnic Inst. and State Univ., Blacksburg, VA, June 1995.

[3]Konstadinopoulos, P., Thrasher, D. F., Mook, D. T., Nayfeh, A. H., and Watson, L., "A Vortex-Lattice Method for General Unsteady Aerodynamics," *Journal of Aircraft*, Vol. 22, No. 1, 1985, pp. 43–49.

[4]Miley, S. J., "A Catalog of Low Reynolds Number Airfoil Data for Wind Turbine Application," Contract No. DE-AC04-76DP03533, Dept. of Aerospace Engineering, Texas A&M Univ., College Station, TX, Feb. 1982.

[5]McCroskey, W. J., McAlister, K. W., Carr, L. W., Pucci, S. L., Lambert, O., and Indergrand, R. F., "Dynamic Stall on Advanced Airfoil Sections," *Journal of the American Helicopter Society*, July 1981, pp. 40–50.

[6]Katz, J., and Plotkin, A., *Low-Speed Aerodynamics: From Wing Theory to Panel Methods*, McGraw–Hill, New York, 1991, Chap. 13.